J3.5 Integration of the total lightning jump algorithm into current operational warning environment conceptual models

C. J. Schultz[1,2], L. D. Carey[2], E. V. Schultz[2], G. T. Stano[3], R. Blakeslee[1], and S. J. Goodman[4]

1 – NASA Marshall Space Flight Center, Huntsville, AL
2- Department of Atmospheric Science, University of Alabama Huntsville, Huntsville, AL
3 – ENSCO/NASA SPoRT, Huntsville, AL
4 – NOAA/NESDIS, Greenbelt, MD

1. Introduction

The purpose of the total lightning jump algorithm (LJA) is to provide forecasters with an additional tool to identify potentially hazardous thunderstorms, yielding increased confidence in decisions within the operational warning environment. The LJA was first developed to objectively indentify rapid increases in total lightning (also termed "lightning jumps") that occur prior to the observance of severe and hazardous weather (Williams et al. 1999, Schultz et al. 2009, Gatlin and Goodman 2010, Schultz et al. 2011). However, a physical and framework leading up to and through the time of a lightning jump is still lacking within the literature. Many studies infer that there is a large increase in the updraft prior to or during the jump, but are not specific on what properties of the updraft are indeed increasing (e.g., maximum updraft speed vs volume or both) likely because these properties were not specifically observed.   Therefore, the purpose of this work is to physically associate lightning jump occurrence to polarimetric and multi-Doppler radar measured thunderstorm intensity metrics and severe weather occurrence, thus providing a conceptual model that can be used to adapt the LJA to current operations.

2. Data and Methodology

This study takes advantage of multiple observational platforms through the use of a well-established polarimetric, multiple Doppler domain and total lightning observations in North Central Alabama (Fig. 1). These unique observations allow for three dimensional (3D) retrievals of velocity and total lightning mapping. Furthermore, polarimetric radar information particle identification provides the volumetric growth/decay of precipitation sized ice (e.g., graupel, ice crystals) necessary for electrification.

One of the primary radars used in this analysis is the University of Alabama in Huntsville's Advanced Radar for Meteorological and Operational Research (ARMOR; Schultz et al. 2012, Knupp et al. 2014). ARMOR is a C-band, polarimetric radar located at the Huntsville International Airport (KHSV). ARMOR operates in simultaneous linear transmit and receive (also known as slant 45), and collects horizontal reflectivity (Z_{HH}), radial velocity (V_r), spectrum width (SW), differential reflectivity (Z_{DR}), correlation coefficient (ρ_{hv}), and differential propagation phase (Φ_{dp}).
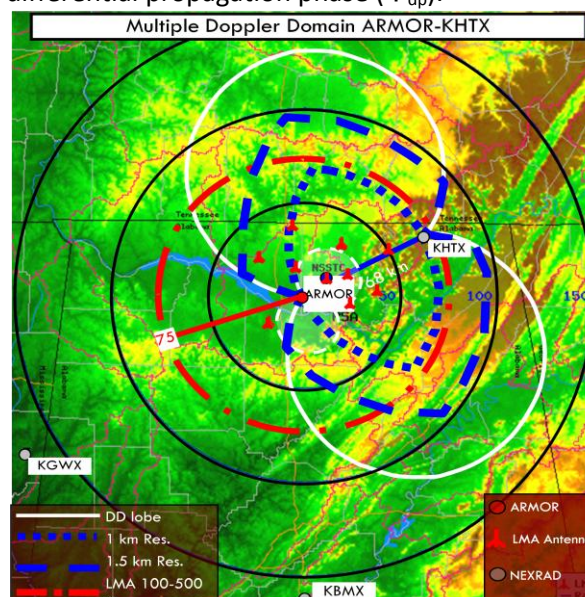

Figure 1: ARMOR-KHTX DD domain (blue outline) and NALMA antenna locations (red markers).

Radar data were corrected for attenuation and differential attenuation (Bringi et al. 2001), and aliased velocities were unfolded using NCAR's SOLO3. Data were then gridded to a Cartesian coordinate system with a Cressman weighting scheme on a grid size of 300 x 300 x 19 using a resolution of 1 km x 1 km x 1 km using NCAR's REORDER (Oye et al. 1995).

Particle identification (PID) was performed using the polarimetric information from ARMOR. NCAR's PID algorithm was utilized and tuned for C-band (Vivekanandan et al. 1999, Deierling et al. 2008). The primary hydrometeor type and property observed is the volume of graupel within the mixed phase region (-10°C to -40°C) where electrification is known to occur.

Multiple Doppler analysis was performed between ARMOR and the Weather Service Radar-88D (WSR-88D) at Hytop, AL (KHTX). In order to retrieve accurate vertical velocities, radar volume times between the two radars were required to occur within 2 minutes of each other. This requirement reduces errors in vertical velocity retrieval. Using NCAR's Custom Editing and Display of Reduced Information in Cartesian Space (CEDRIC; Mohr et al. 1986), dual-Doppler synthesis was performed with a manual input of storm motion. The variational integration technique was used for multi-Doppler synthesis to minimize errors within the retrievals (Matejka and Bartels 1998). This requires that the anelastic continuity equation is integrated from an upper and a lower boundary and vertical motion at these boundaries are set to 0 m s^{-1}. Upward integration from the lower boundary condition occurs in the lowest three vertical levels of the grid space, and downward integration from the upper boundary occurs in the remaining vertical levels.

Three dimensional total lightning information was collected by the NASA's North Alabama Lightning Mapping Array (NALMA, Koshak et al. 2004, Goodman et al. 2005). NALMA is a 11 station array operating between 76-82 MHz that is centered at the National Space Science and Technology Center on the campus of the University of Alabama-Huntsville. The peak power of very high frequency (VHF) radiation source points associated with electrical breakdown are collected every 80 µs. These VHF source points are then recombined using a flash clustering algorithm developed by McCaul et al. (2009) to build flashes. A flash must have a minimum of 10 VHF source points to be considered in this analysis.

Thunderstorms examined in this study were objectively tracked using output from the Thunderstorm Identification Tracking Analysis and Nowcasting algorithm (TITAN; Dixon and Wiener 1993). These objective storm tracks provided a framework in which storm based characteristics (e.g., total flash rate, peak reflectivity, graupel volume, etc.) can be recorded with time, analyzed for trends and intercompared with each other for integrated, multi-platform storm analysis.

Lightning jumps were objectively identified using the 2σ algorithm from Schultz et al. (2009; 2011). This technique uses 14 minutes of the thunderstorm's recent flash rate history to understand if the current behavior of a storm's flash rate is abnormal. As outlined in Schultz et al. (2009, 2011), the algorithm is a 5 step process.

1) The total flash rate from the 14 minute period is binned into 2 minute time periods, and the total flash rate is averaged.
2) The time rate of change of the total flash rate (DFRDT) is calculated by subtracting consecutive bins from each other (i.e., bin_2-bin_1, bin_3-bin_2,… bin_7-bin_6). This results in 6 DFRDT values with the units of flashes min^{-2}.
3) Next the 5 oldest values are used to calculate a standard deviation of the population. Twice this standard deviation value determines the jump threshold.
4) If the remaining newest DFRDT time exceeds the jump threshold, a jump has occurred. A jump ends once DFRDT

drops below 0 flashes min^{-2} as new data are collected.

5) This process is repeated every two minutes as new total lightning flash rates are collected until the storm dissipates.

In order for a jump to be valid, the total flash rate must exceed 10 flashes per minute. This threshold is used to mitigate smaller jumps in total lightning that commonly occur in ordinary convective storms (i.e., non-severe).

The convective morphology of storms within this study includes isolated ordinary storms, multicellular convection, supercells (including tropical and low echo centroid storms), and quasi-linear convective systems (QLCS). The purpose behind examining this spectrum of storms is to understand not only the physics and energetic of severe storms, but also to understand what typically occurs in ordinary convection. A total of 18 events, with over 30 individual storms are used in this study; however, for this specific paper, only 3 lightning jumps will be discussed in detail.

3. Results

The following observations presented are from 3 jumps during which multiple Doppler, polarimetric and 3D total lightning coverage were all available. These three events include a non-tornadic supercell, a QLCS that produces copious amounts of large hail, and a typical multicellular severe storm that produces wind damage during the summer months. Two of these jumps occur during the development stages of the severe convection (supercell, QLCS) while the third occurs after the convection has already matured.
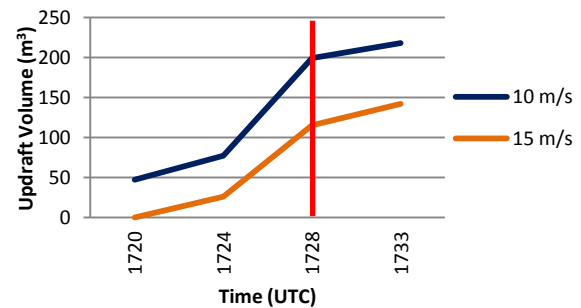
3a. April 10, 2009

A number of supercells pounded the Southeastern US with severe weather on this day. Specifically in the Tennessee Valley, at least 8 supercell storms produced hail to the size of baseballs, and 1 EF3 tornado. The storm
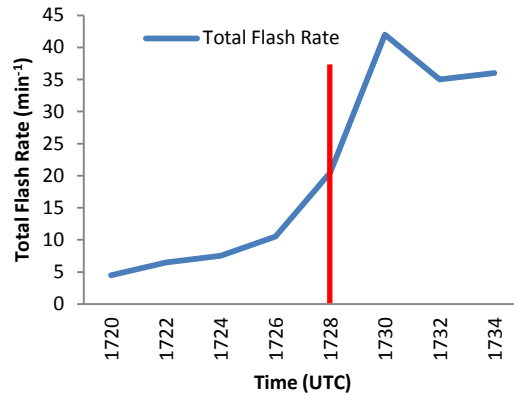

Figure 2: Total flash rate from the non-tornadic supercell at the time of the first lightning jump at 1728 UTC (red bar).

examined here did not produce a tornado, but did produce hail up to 1.75 inches in diameter.

The storm specifically studied is ideal for analysis because the first objectively identified 2σ lightning jump with this storm occurs at 1728 UTC as it transitioned from a non-severe convective element into a full-fledged supercell. Figure 2 shows the rapid increase in total lightning that occurs at 1728 UTC. Here the total flash rate explodes from 10 flashes per minute to 40 flashes per minute within a span of 4 minutes. During this same period, dual Doppler analysis reveals that the 10 and 15 m s^{-1} updraft volume also increases dramatically during this period (Fig. 3).

Figures 4a-c show the 3 dual-Doppler times leading up to the lightning jump occurrence. At 1720 UTC the updraft at 6 km is fairly typical for an ordinary (i.e., non-severe) thunderstorm

Figure 3: 10 and 15 m s^{-1} updraft volume at the time of the first lightning jump (red bar) in the non-tornadic supercell on April 10, 2009.
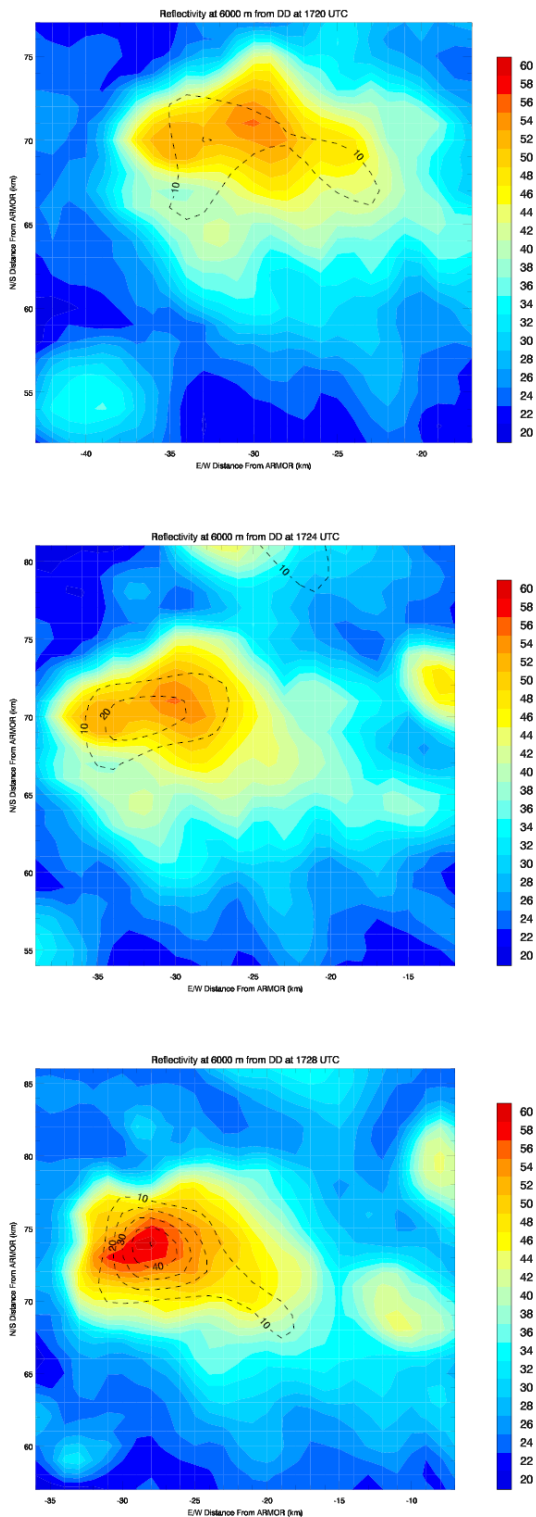
Figure 4: Z_{HH} and updraft speed at 6 km from the ARMOR-KHTX dual-Doppler for the three times periods leading up to the lightning jump (1720, a, top; 1724, b, middle; and 1728, c, bottom).

with a peak magnitude just over 10 m s^{-1} (Fig. 3a). By 1724 UTC, the peak updraft magnitude has increased significantly within the mixed phase region, now just over 20 m s^{-1} (Fig. 4b). By 1728 UTC the updraft has increased again by a factor of 2 to over 40 m s^{-1} (Fig. 3c). These three panels also indicate that Z_{HH} has also increased at this level during the same time period, which corresponds with the theory that an increase in precipitation-sized ice within the mix phase region enhanced charging and ultimately lightning production (e.g., Carey et al. 2000, Deierling et al. 2008). Furthermore, the storm's mesocyclone developed immediately after the lightning jump (Stough et al. 2014), and a lightning hole was present 5 minutes after the lightning jump (Kozlowski and Carey 2014).
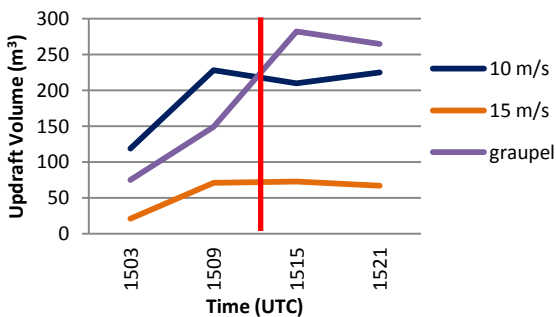
3b. March 12, 2010

A QLCS on the morning of March 12, 2010 produced copious amounts of hail and high winds across Marshall, Jackson and Dekalb Counties in Alabama. Damage included many trees down, windows blown out and holes in siding from hail being driven into the sides of homes. The portion of the QLCS responsible for the damaging wind and hail swath intensified as it entered the ARMOR-KHTX dual-Doppler domain at 1500 UTC.

The first 2σ lightning jump occurred within the damaging portion of the QLCS occurred at 1512 UTC. Here the total flash rate increased from 16 flashes per minute to 35 flashes per minute in two minutes (Fig. 5). Updraft volumes also spiked during this period from 119 km^3 to 228 km^3 for 10 m s^{-1} updraft volume and 21 km^3 to 71 km^3 for 15 m s^{-1} updraft volume (Fig. 6). Also seen in Fig. 6 is the spike in inferred graupel volume within the mixed phase region (-10°C to -40°C) near the time of the lightning jump. Graupel volume increased dramatically, from 75 km^3 at 1503 UTC to 282 km^3 by 1515 UTC. Interestingly, the maximum updraft speed did not increase, but remained steady between 1503 and 1515 UTC, with a value of 21 m s^{-1} (Fig. 7).
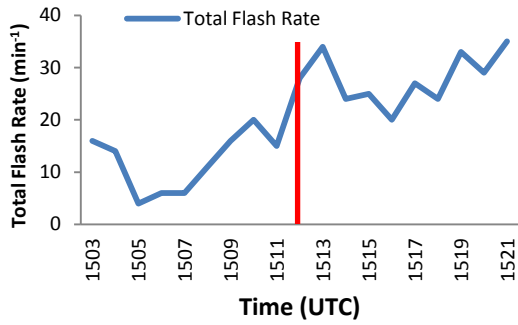
Figure 5: Total flash rate vs time from the severe QLCS on March 12, 2010. First jump occurs at 1512 UTC (red bar).

It is unclear at this point the exact reasoning why the peak updraft remained constant and did not increase during the period leading up to the jump like in *3a.*, and further interrogation of the storm is necessary. However, the lack of an increase in the peak updraft at the time of the lightning jump is not surprising because the particles responsible for charge separation have typical fall speeds less than 5-10 m s^{-1}. Thus, within a region of peak updraft (e.g., > 20 m s^{-1}) hydrometeors have a short residence time that inhibits precipitation growth and charging from rebounding collisions between riming graupel and cloud ice (e.g., MacGorman et al. 2008, Kozlowski and Carey 2014). Updraft volumes (e.g., 10 or 15 m s^{-1}) have more control on the ability for the storm to levitate because fall speeds of the precipitation ice-sized particles needed to

Figure 6: 10 and 15 m s^{-1} updraft and graupel volume at the time of the first lightning jump (red bar) in the severe portion of the QLCS on March 12, 2010.
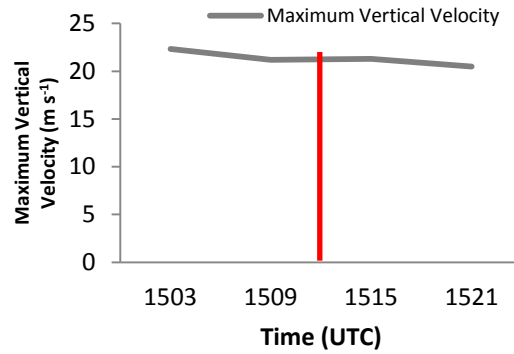
Figure 7: Maximum vertical velocity at the time of the first lightning jump in severe portion of the QLCS on March 12, 2010.

facilitate development of a strong electric field capable for electrical breakdown are similar, allowing for longer residence times. This hypothesis is also corroborated by previous studies that show that peak updraft speed is not always well correlated with the total flash rate (e.g., Kuhlman et al. 2006, Deierling et al. 2008).

Two additional jumps were observed within this section of the QLCS at 1550 UTC and 1602 UTC (not shown). Numerous hail reports between 0.75-1.75 inches were reported across Northeast AL between 1500-1700 UTC and the amount of hail was so great that hail remained on the ground for several hours after the event.

3c. July 19, 2006

The thunderstorms on the afternoon of July 19, 2006 were fairly typical for the summer time across the Southeast US, where the main threat from the strongest storms of the day would be high winds. The multicellular thunderstorm examined here developed near Fayetteville, TN, and eventually produced wind damage within city limits. Unfortunately, the volumetric coverage from ARMOR was not available for the first two lightning jumps
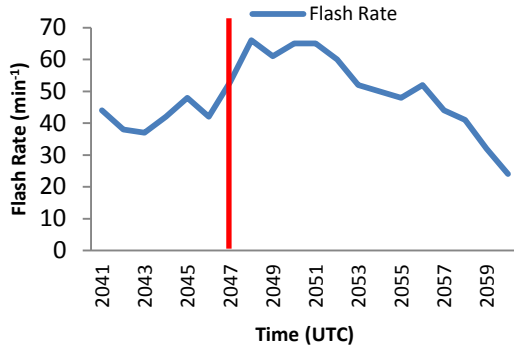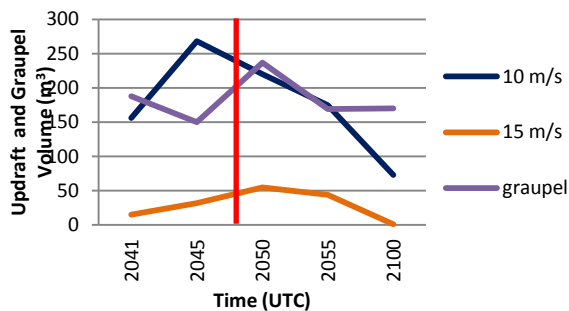
Figure 8: Total flash rate from a multicellular thunderstorm on July 19, 2006. The third jump from this storm occurs at 2047 UTC.

Figure 10: Maximum vertical velocity at the time of the third lightning jump (red bar) a multicellular severe storm from July 19, 2006.
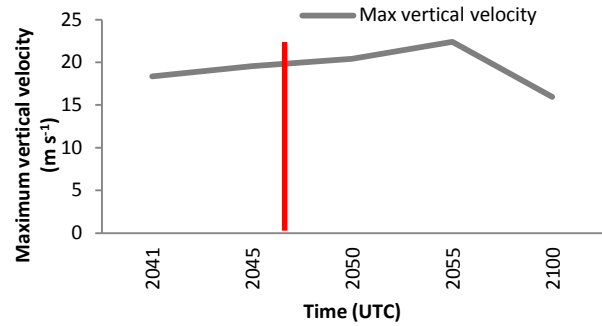
associated with this storm, however, ARMOR began scanning the storm at 2041 UTC, just prior to the observance of a third jump and subsequent severe weather.

At 2041 UTC when ARMOR volumetric scans began on the storm, the peak flash rate was already at 44 flashes per minute (Fig. 8). At 2045 UTC the flash rate had increased modestly to 48 flashes per minute; however, by 2050 UTC, the total flash rate had peaked at 65 flashes per minute. A lightning jump occurred in between these two volume times at 2047 UTC.

Similar behavior in updraft volume was observed to the previous two cases in which the first lightning jumps with those storms were analyzed. Figure 9 shows that both 10 and 15 m s^{-1} updraft volumes increased leading up to the jump time at 2047 UTC. Here 10 m s^{-1} updraft volume increases from 156 km^3 at 2041 UTC to 268 km^3 at 2045 UTC. Similarly, 15 m s^{-1}

updraft volume increased from 15 km^3 at 2041 UTC to 32 km^3 at 2045 UTC, eventually peaking at 51 km^3 at 2050 UTC. Unlike the March 12, 2010 case, graupel volume fell from 188 km^3 to 150 km^3 between 2041 and 2045 UTC before increasing once again at 2050 UTC to 237 km^3. Finally, maximum updraft speed remained steady at 20 m s^{-1} leading up to and through the lightning jump (Fig. 10). Importantly, this final jump occurred prior to the manifestation of damaging winds at the surface that were observed between 2050 and 2108 UTC.

4. Summary and Future work

The results presented above highlight the following observations at the time of the lightning jumps analyzed:

1) Increases in 10 and 15 m s^{-1} updraft volume are observed leading up to the time of the lightning jump.
2) Maximum velocity does not always increase in magnitude leading up to the jump, and can remain steady in magnitude or even decrease slightly. This observation is not surprising because updraft volumes have more control on the ability for the storm to levitate precipitation ice-sized particles to facilitate precipitation growth and development of a strong electric field capable for electrical breakdown than solely the peak updraft speed. Short

Figure 9: 10 and 15 m s^{-1} updraft and graupel volume at the time of the third lightning jump (red bar) a multicellular severe storm from July 19, 2006.

residence time of hydrometeors through the mixed-phase region in a region of peak updraft (> 20 m s^{-1}) inhibits precipitation growth and of charging from rebounding collisions between riming graupel and cloud ice (e.g., MacGorman et al. 2008, Kozlowski and Carey 2014).

3) Graupel volume is shown to increase dramatically with the total flash rate, but can lag the increase in updraft volume.

Future work will continue to drive home the physical and dynamical understanding behind lightning jump occurrence through coupling of each jump with additional thunderstorm intensity metrics. This fusion of intensity metrics will increase the utility of the lightning jump within the operational severe storm warning environment.

5. References

Bringi, V.N., T.D. Keenan, V., Chandrasekar, 2001: Correcting C-Band radar reflectivity and differential reflectivity data for rain attenuation: A self-consistent method with constraints. *IEEE Trans. on Geo. and Rem. Sens.*, **39**, 1906-1915.

Carey, L. D. and S. A. Rutledge, 2000: On the relationship between precipitation and lightning in tropical island convection: A C-band polarimetric radar study. *Mon. Wea. Rev.*, **128**, 2687-2710.

Deierling, W., W. A. Petersen, J. Latham, S. Ellis, and H. J. Christian, 2008: The relationship between lightning activity and ice fluxes in thunderstorms. *J. Geophys. Res.*, **113**, D15210, doi:10.1029/2007JD009700.

Deierling, W. and W. A. Petersen, 2008: Total lightning activity as an indicator of updraft characteristics. *J. Geophys. Res.*, **113**, doi:10.1029/2007JD009598.

Gatlin, P. N. and S. J. Goodman, 2010: A total lightning trending algorithm to identify severe thunderstorms. *J. Atmos. Oceanic Technol.*, **27**, 3-22.

Goodman, S. J. and Coauthors, 2005: The North Alabama Lightning Mapping Array: Recent severe storm observations and future prospects. *Atmos. Res.*, **76**, 423-437.

Goodman, S. J., and Coauthors, 2013: The GOES-R Geostationary Lightning Mapper (GLM). *Atmos. Res.*, **125-126**, 34-49.

Koshak, W. J. and Coauthors, 2004: North Alabama Lightning Mapping Array (LMA): VHF source retrieval algorithm and error analysis. *J. Atmos. Ocean. Tech.*, **21**, 543-558.

Kozlowski, D. M., and L. D. Carey, 2014: An Analysis of Lightning Holes in Northern Alabama Severe Storms Using a Lightning Mapping Array and Dual-Polarization Radar. *Preprints 5th ILMC*, Tuscon, AZ. Vaisala.

Knupp, K. R., and Coauthors, 2014: Meteorological Overview of the Devastating 27 April 2011 Tornado Outbreak. *Bull. Amer. Meteorol. Soc.*, in press, doi: http://dx.doi.org/10.1175/BAMS-D-11-00229.1

Kuhlman, K. M., C. L. Ziegler, E. R. Mansell, D. R. MacGorman, and J. M. Straka, 2006: Numerically simulated electrification and lighting of the 29 June STEPS supercell storm. *Mon. Wea. Rev.*, **134**, 2734-2757.

MacGorman and Coauthors (2008), TELEX: The Thunderstorm Electrification and Lightning Experiment. *Bull. Amer. Meteor. Soc.*, **89**, 997-1013.

McCaul, E. W, Jr., S. J. Goodman, K. M. LaCasse, and D. J. Cecil, 2009: Forecasting lightning threat using cloud-resolving model simulations. *Wea. Forecasting*, **24**, 709-729.

Matejka, T. and D. L. Bartels, 1998: The accuracy of vertical air velocities from Doppler radar data. *Mon. Wea. Rev.*, **92**, 92-117.

Mohr, C. G., L. J. Miller, R. L. Vaughn, and H. W. Frank, 1986: The merger of mesoscale data sets into a common Cartesian format for efficient and systematic analysis. *J. Atmos. Ocean. Technol.*, **3**, 143-161.

Oye, D. and M. Case, 1995: REORDER: A program for Gridding Radar Data. Installation and User Manual for the UNIX Version. NCAR Atmospheric Technology Division, Boulder, CO, 19 pp.

Schultz, C. J., W. A. Petersen, and L. D. Carey, 2009: Preliminary development and evaluation of lightning jump algorithms for the real-time detection of severe weather. *J. Appl. Meteor.*, **48**, doi:10.1175/2009JAMC2237.1.

Schultz, C. J., W. A. Petersen, and L. D. Carey, 2011: Lightning and severe weather: A comparison between total and cloud-to-ground lightning trends. *Wea. and Forecasting*, **26**, 744-755, doi:10.1175/WAF-D-10-05026.1.

Schultz, C. J. and Coauthors, 2012a: Dual-polarization tornadic debris signatures Part I: Examples and utility in an operational setting. *Electronic J. Operational Meteor.*, **13**, 120-137.

Stough, S. M., L. D. Carey and C. J. Schultz, 2014: Total lightning as an indicator of mesocyclone behavior. *Preprints 26th Conf. on Wea. Analysis and Forecasting*, Atlanta, GA. Amer. Met. Soc.

Straka, J. M., D. S. Zrnic, and A. V. Ryzhkov, 2000: Bulk hydrometeor classification and quantification using polarimetric radar data: Synthesis of relations. *J. Appl. Meteorol.*, **39**, 1341-1372.

Vivekanandan, J., D. S. Zrnic, S. M. Ellis, R. Oye, A. V. Ryzhkov, and J. Straka, 1999: Cloud microphysics retrieval using S-band dual-polarization radar measurements. *Bull. Amer. Meteorol. Soc.*, **80**, 381-388.

Williams, E. R. and Coauthors, 1999: The behavior of total lightning activity in severe Florida thunderstorms. *Atmos. Res.*, **51**, 245-265.